ANTIOXIDANTS & REDOX SIGNALING
Volume 1, Number 1, 1999
Mary Ann Liebert, Inc.

Inhibition of the Insulin Receptor Kinase Phosphorylation by Nitric Oxide: Functional and Structural Aspects

ELMAR SCHMID,[1] AGNES HOTZ-WAGENBLATT,[2] and WULF DRÖGE[1]

ABSTRACT

Previous studies on cultured skeletal muscle cells have indicated that the insulin-induced expression of GLUT4 transporter protein is inhibited by nitric oxide (NO). Therefore, we determined the effect of NO on the insulin-induced autophosphorylation of the insulin receptor kinase (IRK), *i.e.*, the first step in the insulin-mediated signal transduction pathway. The experiments showed that the insulin-induced autophosphorylation of the insulin receptor β-chain is strongly inhibited by the NO donors 1,1-diethyl-2-hydroxy-2-nitrosohydrazine (DEA-NO) or *S*-nitroso-*N*-acetylpenicillamine (SNAP). The inhibitory effect was ameliorated in cells depleted of glutathione (GSH), suggesting the possibility that *S*-nitroso-glutathione may operate as an intermediate NO donor. Complementary experiments with different Cys → Ala mutant proteins showed, surprisingly, that all mutant proteins were inhibited by DEA-NO. Three-dimensional models of the nonphosphorylated IR β-chain nitrosylated at the accessible cysteine residues 1056, 1138, 1234, or 1245 revealed that derivatization of any of these four cysteine residues leads essentially to the same structural changes of the IRK domain. These changes involve a movement of the amino-terminal lobe against the carboxy-terminal lobe in a direction opposite to the direction of the "lobe closure" that was previously proposed to facilitate the accessibility for ATP and the expression of catalytic activity. Our findings suggest that the occurrence of several functionally relevant cysteine residues in distinct regions of the IRK protein increases the probability of regulatory redox interactions and thus the redox sensitivity of the IRK. Antiox. Redox Signal. 1, 45–53.

INTRODUCTION

An abnormally low insulin receptor kinase (IRK) activity and accordingly low insulin responsiveness of the skeletal muscle tissue are common findings in obesity, non-insulin-dependent diabetes mellitus (NIDDM) and old age (Cahill, 1971; Friedenberg *et al.*, 1987; Takayama *et al.*, 1988; Fukagawa *et al.*, 1989; Damsbo *et al.*, 1991; Carvalho *et al.*, 1996). The underlying mechanism is still poorly understood. However, a recent study on cultured skeletal muscle cells indicated (i) that the insulin-induced expression of the GLUT4 transporter protein is substantially inhibited by the cytokine combination tumor necrosis factor-α (TNF-α) plus interferon-γ (IFN-γ), which induces nitric oxide synthase (iNOS) and (ii) that this inhibition is prevented by the iNOS inhibitor N^G-nitro-L-arginine methyl ester (L-

[1]Division of Immunochemistry, and [2]Division of Molecular Biophysics, Deutsches Krebsforschungszentrum, D-69120 Heidelberg, Germany.

NAME) (Bédard *et al.*, 1997). In addition, NO was shown to inhibit the epidermal growth factor receptor tyrosine kinase (Estrada *et al.*, 1997) and to modulate the function of several other enzymes and cell signal proteins by *S*-nitrosylation of critical cysteine residues (Lei *et al.*, 1992; Molina *et al.*, 1992; Stamler *et al.*, 1992; Caselli *et al.*, 1994; Stamler, 1994; Becker *et al.*, 1995; Lander *et al.*, 1996). Therefore, we investigated the possibility that activation of the IRK may be compromised by NO.

Binding of insulin to the IR activates the tyrosine kinase by inducing the autophosphorylation of Tyr1162, Tyr1163, and Tyr1158 in the activation loop of the IR β-chain (β-1R) (reviewed in Lee and Pilch, 1994; Taylor *et al.*, 1995). The comparison of the crystal structures of the nonphosphorylated IRK-0P (Hubbard *et al.*, 1994) and the phosphorylated IRK-3P (Hubbard, 1997) indicated that autophosphorylation is associated with a dramatic change in the three-dimensional structure of the IRK domain. Specifically, autophosphorylation induces a reorientation of the amino- and carboxy-terminal lobes of the kinase that is necessary for productive ATP binding. When the carboxy-terminal lobes of IRK and IRK-3P were superimposed, a nearly pure rotation of the amino-terminal lobe of IRK by about 21° was found to line the five-stranded β-sheets (Hubbard, 1997). This reorientation was described as "lobe closure" and was shown to provide a greater accessibility of the ATP binding site. We used functional studies in combination with molecular modeling to characterize the effects of NO.

MATERIALS AND METHODS

Induction of autophosphorylation by insulin

CHO-hIR cells were routinely cultured in F12 medium with 10% fetal calf serum (FCS), glutamine, and antibiotics. Before each experiment, the cells were incubated in modified NCTC 135 medium (Eck *et al.*, 1989) for 17 hr under serum-free conditions, and finally incubated for 30 min with the indicated concentrations of 1,1-diethyl-2-hydroxy-2-nitrosohydrazine (DEA-NO), or *S*-nitroso-*N*-acetylpenicillamine (SNAP) (Molecular Probes, Eugene, OR) plus 12 min with human recombinant insulin (SIGMA) (100 n*M*) as indicated. If indicated, the NCTC 135 medium was supplemented with 30 μ*M* buthionine-sulfoximine (BSO), *i.e.*, a specific inhibitor of glutathione biosynthesis (Griffith and Meister, 1979) to deplete intracellular GSH. The cells were lysed. If indicated, the IR was immunoprecipitated with the monoclonal hIR β-chain antibody Ab-1 (Oncogene Science) as described (Schmid *et al.*, 1998). Aliquots of the lysates or immunoprecipitates containing equal amounts of protein were subjected to SDS-PAGE and Western blotting and were finally probed for tyrosine phosphorylation of the IR β-chain with the monoclonal antiphosphotyrosine antibody 4G10 (Upstate Biotechnology Inc. BioMol, Hamburg, Germany) and for IR expression with a polyclonal anti-βIR antibody (Santa Cruz, Heidelberg) as described (Schmid *et al.*, 1998).

Immunoprecipitated IR was also tested for *in vitro* autophosphorylation with [γ-^{32}P]ATP (*in vitro* kinase assay) as described (Schmid *et al.*, 1998). Glutathione (GSH) and protein were determined as described (Eck *et al.*, 1989).

Expression of IR mutant proteins

pECE expression vectors of the human β-IR containing the single mutations Cys981Ala, Cys1056Ala, Cys1138Ala, Cys1234Ala, Cys1245Ala, and Cys1308Ala (Macaulay *et al.*, 1995) and the corresponding wild-type hIR DNA were kindly provided by Dr. C.W. Ward (CPIRO, Parkville, Australia). We have confirmed the Cys1138Ala mutation by DNA sequencing. Plasmids were transformed into *Escherichia coli* strain DH5a (Clontech). After quantitative plasmid preparation (Quiagen), the *Xbal–Bam*HI fragment was prepared to confirm the wild-type and mutated hIR DNA. Chinese hamster ovary (CHO) cells were transiently transfected with 2 μg of wild-type or mutated hIR DNA using the lipofectamine technique (Gibco/BRL) according to the manufacturer's protocol. The cells were then cultured for 2 days in F12 medium and subsequently incubated in serum-free modified NCTC 135 medium for another 17 hr and treated as described above.

Modeling of three-dimensional structures

The three-dimensional structures of the IR kinase domain and its various derivatives and mutants were modeled on an Indigo II workstation (Silicon Graphics). The starting coordinates of nonhydrogen atoms were taken from the Protein Data Bank (PDB) entry 1 irk (Hubbard *et al.*, 1994). Atoms not reported in PDB 1 irk were inserted with the help of the INSIGHT II library, and hydrogen atoms were added (see Figs. 4 and 5, upper panels; ethyl-mercury groups not shown). This structure (1 irk) was the basis for all subsequent modifications. Energy minimization was performed on an IBM-SP2 workstation using the DISCOVER module of the INSIGHT II program (Molecular Simulation BIOSYM Technologies INC.) and the conjugate gradient method for energy minimization. The generation of hydrogen atoms and the automatic assignment of atom potential types and partial charges were achieved using the consistent valence forcefield (CVFF) (Hagler and Lifson, 1974). The polar amino acids of the molecule were in the uncharged form and a dielectric constant of 1 was used because the water in the electrostatic environment was expected to inhibit interactions at the surface. During the first 100 steps of minimization, only the hydrogen atoms were allowed to move to avoid large forces at the backbone just because of the newly added hydrogens. For the next 100 steps of geometry optimization, all Cα atoms were tethered using a harmonic potential with the force constant of 100 kJ. Full minimization of all atoms was finally carried out until the maximum force value reached a value below 0.001. The figures of the minimized structures were obtained by RASMOL (Roger Sayle).

RESULTS

Inhibition of the insulin-stimulated IR autophosphorylation by NO donors

To determine the effect of NO on the IRK activity, we incubated CHO-hIR cells with two different NO donors, *i.e.*, DEA-NO or SNAP. These experiments showed that the autophosphorylation of the β-IR is strongly inhibited in a dose-dependent way by both NO donors (Fig. 1). Western blots confirmed that the level of β-IR expression was not significantly affected by the NO donors. The inhibitory effect of DEA-NO has also been confirmed by the *in vitro* kinase assay using [γ-^{32}P]ATP (Fig. 2).

The inhibitory effect of NO is facilitated by GSH

To determine whether the NO-mediated inhibition is influenced by the intracellular level of glutathione, we pretreated the cells with buthionine sulfoximine (BSO), a specific inhibitor of GSH biosynthesis (Griffith and Meister, 1979) prior to treatment with DEA-NO and insulin. A series of control experiments showed that BSO treatment decreased the intracellular GSH level typically from 35.2 ± 3.8 to 3.2 ± 0.7 nmol/mg protein. This depletion of GSH was found to reverse the DEA-NO-mediated inhibition and even enhanced the autophosphorylation of the IR (Fig. 2).

Effect of NO on different Cys → Ala mutant IR proteins

In view of a series of earlier reports that the functions of proteins may be positively or neg-

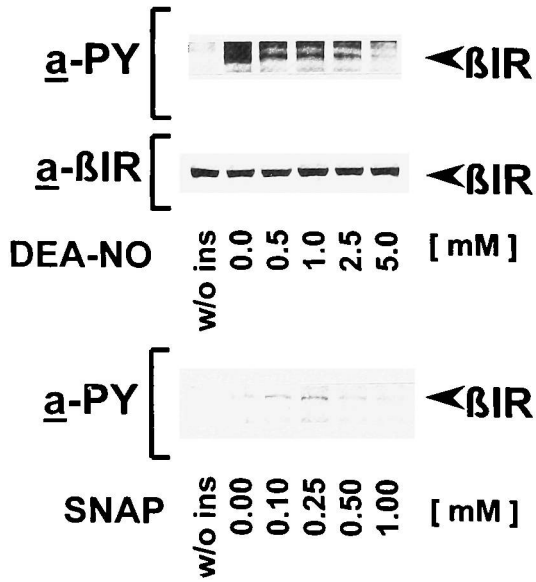

FIG. 1. Inhibition of insulin-stimulated IR autophosphorylation by different NO donors. CHO-HIR cells were incubated with the indicated graded concentrations of DEA-NO or SNAP and subsequently stimulated with insulin. Aliquots of the whole-cell lysates were assayed for β-IR phosphorylation (α-PY) and IRK expression (α-βIR) as described in the Materials and Methods section.

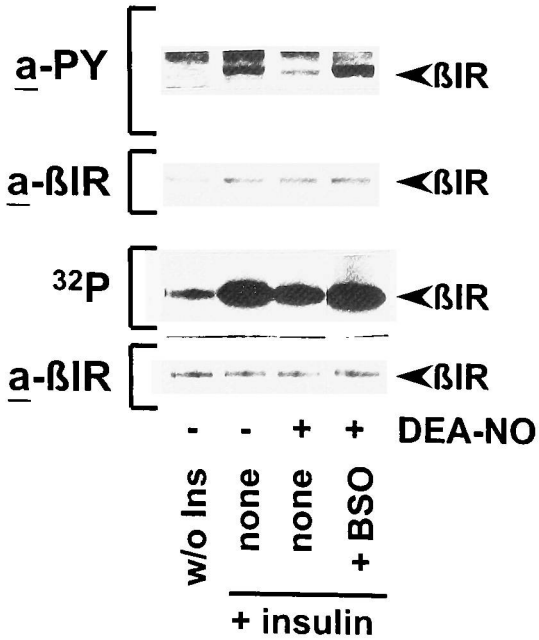

FIG. 2. **Role of glutathione in the inhibitory effect of NO.** *Upper panels.* CHO-HIR cells were incubated overnight in modified NCTC 135 medium (Eck *et al.*, 1989) with or without 30 μM BSO as indicated. They were then incubated for another 30 min with 5 m*M* DEA-NO and, after washing, for another 12 min with 100 n*M* insulin. For other details see legend to Fig. 1. *Lower panels.* Autophosphorylation of immunoprecipitated IR preparations was determined *in vitro* by the kinase assay using [γ-^{32}P]ATP as described (Schmid *et al.*, 1998).

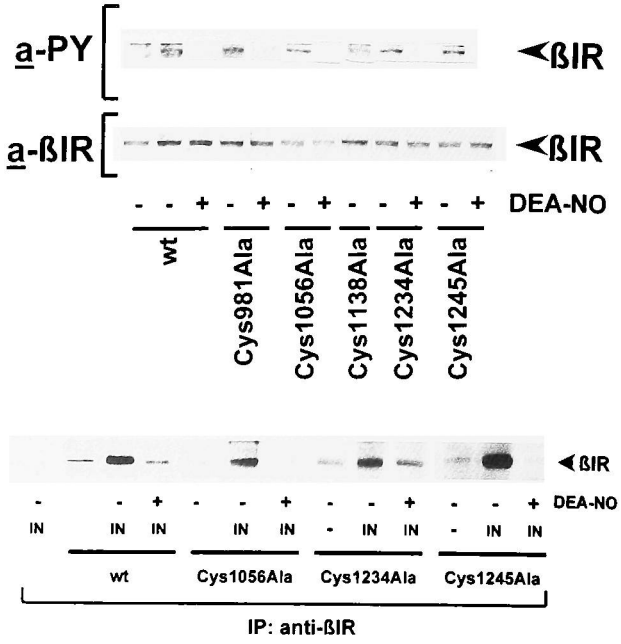

FIG. 3. **Effect of NO on different Cys → Ala mutant IR proteins.** CHO cells were transiently transfected with wild-type or mutated hIR DNA as described in the Materials and Methods section, and incubated for another 2 days in F12 medium. Then they were transferred to NCTC and treated sequentially with DEA-NO and insulin as described in the Materials and Methods section. *Upper panel:* Total lysates were probed with anti-phosphotyrosine antibody. The first lane is a control without insulin. *Lower panel:* Immunoprecipitated preparations of wild-type or mutated IR were probed with anti-phosphotyrosine antibody.

atively altered by *S*-nitrosylation of critical cysteine residues (Lei *et al.*, 1992; Molina *et al.*, 1992; Stamler *et al.*, 1992; Caselli *et al.*, 1994; Stamler 1994; Becker *et al.*, 1995; Lander *et al.*, 1996), we investigated also the effect of NO on different Cys → Ala mutant proteins. CHO cells were in this case transiently transfected with wild-type or mutated hIR DNA and incubated for 2 days in F12 medium prior to transfer to the modified NCTC 135 medium. The cells were then incubated with or without DEA-NO and finally stimulated with insulin as described. Preliminary experiments showed that the mutant Cys1138 Ala had *a priori* already a relatively weak and in most experiments barely detectable activity as tested by antiphosphotyrosine antibody (see Fig. 3, upper

FIG. 4. **Three-dimensional models of the original and S-nitrosylated β-IR.** The view is into the putative ATP binding site. The three-dimensional structures of the IR kinase domain and its derivatives were modeled as described in the Materials and Methods section. The starting coordinates of nonhydrogen atoms were taken from the Protein Data Bank (PDB) entry 1 irk (Hubbard *et al.*, 1994). The structure 1 irk was the basis for all subsequent modifications. Atoms not reported in PDB 1 irk were inserted with the help of the INSIGHT II library and hydrogen atoms were added. The sequence beyond Lys1264 has been deleted because it is relatively unstructured and expected to be flexible in solution. Figures 4 and 5 show the three-dimensional models from three different angles. Figure 4 shows the catalytic site with Tyr1162 (C in grey, O in red, N in blue, H in white) in the upper right corner and its OH group pointing toward the center. The figures show also the catalytic amino acid Asp1132 next to Tyr1162, the Cys residues 1056, 1138, 1234, and 1245, Glu1047 (white), Asn1137 (flesh), and Arg1243 (dark blue). Parts of the backbone are blue (996–1,031), yellow (1,038–1,066), green (1,106–1,125), flesh (1,126–1,145 including the catalytic loop), orange (1,146–1,171 including the activation loop), light grey (1,188–1,235), and pink (1,236–1,245). 1 irk w/o mercury. Three-dimensional model of the wild-type β-IR obtained from 1 irk by deleting the two ethyl-mercury groups and subsequent energy minimization. The structures 1056 Cys-NO, 1138 Cys-NO, 1234 Cys-NO, and 1245 Cys-NO were obtained from 1 irk by replacing the corresponding SH group by a S-NO group.

1 irk

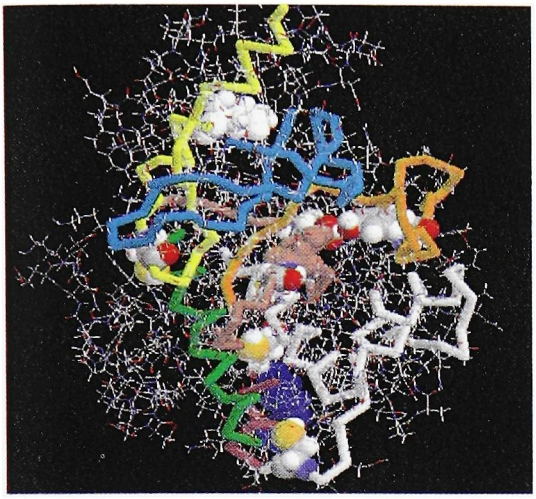

1 irk w/o mercury

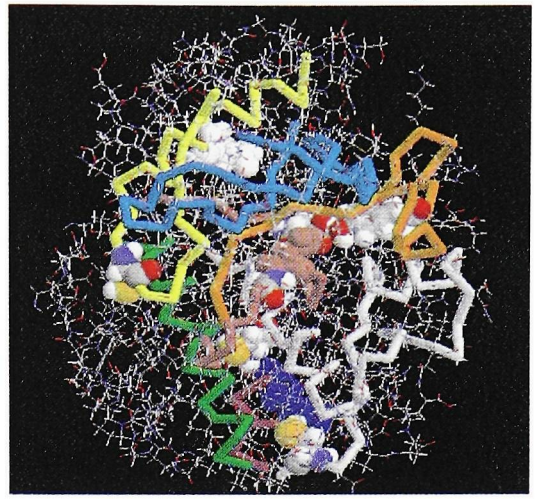

1056 Cys-NO

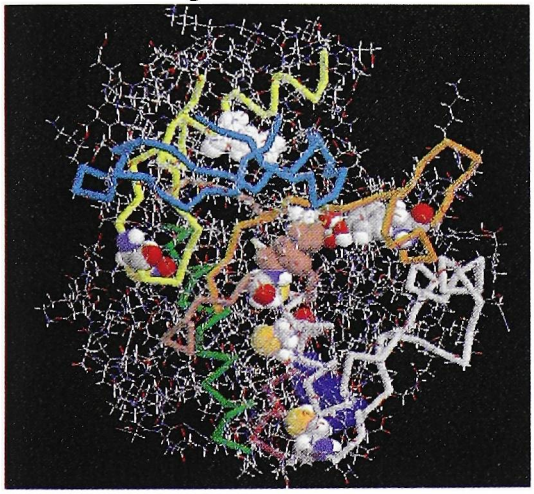

1138 Cys-NO

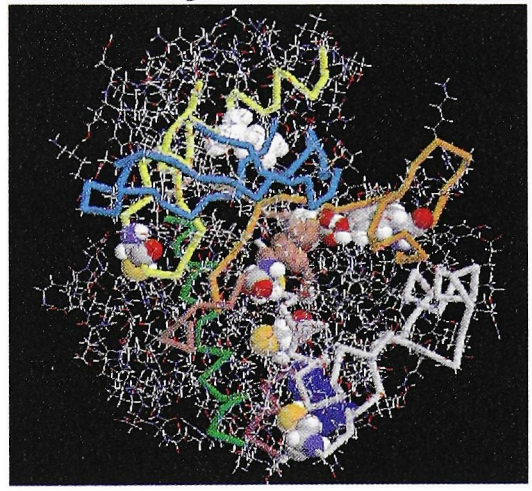

1234 Cys-NO

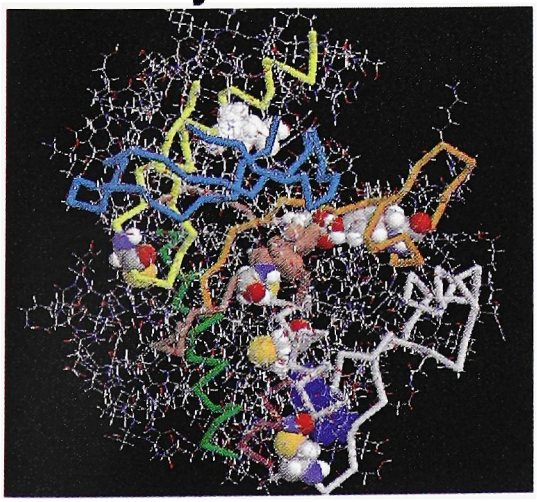

1245 Cys-NO

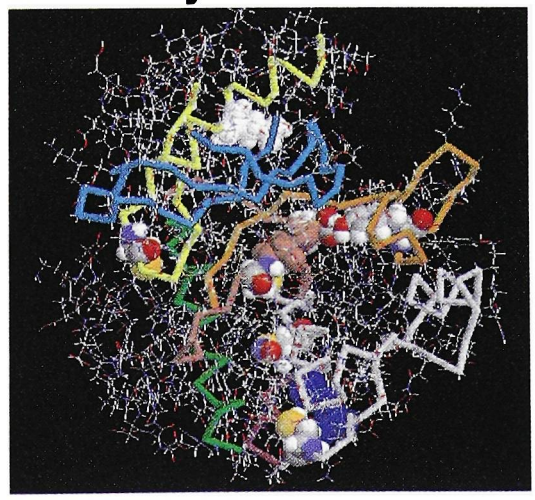

panel) or by the *in vitro* kinase assay with [γ-^{32}P]ATP (not shown). All other cysteine mutants under test were tested for inhibition by DEA-NO and were found to be equally sensitive to inhibition by NO (Fig. 3). This inhibition was demonstrable in lysates (Fig. 3, upper panel) as well as in immunoprecipitated IR preparations (Fig. 3, lower panel).

Three-dimensional models of the S-nitrosylated β-IR

In view of the unexpected finding that mutation of any of the individual cysteine residues of the IRK β-chain did not prevent the NO-mediated inhibition of the IRK, we analyzed the effect of *S*-nitrosylation of individual cysteine residues by molecular modeling techniques. The structure 1 irk w/o mercury (Figs. 4 and 5, upper panels) was ob-tained from the three-dimensional structure of the IRK domain (PDB, 1 irk, see Hubbard *et al.*, 1994) by removing the ethyl-mercury groups and by subsequent energy minimization. The three-dimensional structure Ser981Cys, which was obtained by replacing serine 981 with the authentic cysteine followed by energy minimization, was virtually identical to the structure "1 irk w/o mercury" (not shown). NO was previously shown to convert cysteine residues into *S*-nitrosylated cysteine derivatives (Cys-NO; see Stamler, 1994). The three-dimensional model of 981 Cys-NO (not shown) had essentially the same structure as "1 irk w/o mercury," whereas 1056 Cys-NO, 1138 Cys-NO, 1234 Cys-NO, and 1245 Cys-NO showed a conspicuous dislocation of the entire amino-terminal lobe in relation to the carboxy-terminal lobe. This is illustrated by the movement of the β-sheets β1, β2, and β3 (blue backbone in Figs. 4 and 5) relative to the lower part of the molecule. Most surprisingly, derivatization of any of the four cysteine residues was found to cause almost exactly the same change in the three-dimensional structure. This change causes a reorientation in a direction opposite to the direction of the lobe closure that is believed to be required for optimal ATP binding activity and full catalytic activity of the IRK domain (Hubbard, 1997)

DISCUSSION

Our experiments have shown that the autophosphorylation of the β-IR, *i.e.*, a critical step in the activation of the IRK activity, is strongly inhibited by NO. This finding confirms and extends earlier studies of Bédard and colleagues indicating that NO inhibits the insulin-induced expression of the GLUT4 transporter (Bédard *et al.*, 1997). The results are also in line with a series of earlier reports showing that NO modulates the functional activities of various proteins by *S*-nitrosylation of critical cysteine residues (Lei *et al.*, 1992; Molina *et al.*, 1992; Stamler *et al.*, 1992; Caselli *et al.*, 1994; Stamler, 1994; Becker *et al.*, 1995; Lander *et al.*, 1996). However, not all tyrosine kinase species are inhibited by NO. Unlike the IRK, the Src-family tyrosine kinase p56^{lck} was found to be activated by different NO donors (Lander *et al.*, 1993), whereas the epidermal growth factor receptor tyrosine kinase was again inhibited by NO (Estrada *et al.*, 1997). In view of the marked sequence homology and structural similarity of the catalytic domains of these different tyrosine kinase species, it will be of interest to compare the structural consequences of *S*-nitrosylation in these proteins.

The amelioration of the inhibitory effect by pretreatment with buthionine sulfoximine (BSO) suggests that the intracellular GSH level plays an important role in the NO-mediated inhibition. GSH is known to convert NO into *S*-nitrosoglutathione, *i.e.*, a NO donor that has a much longer half-life than NO itself (Stamler, 1994). *S*-Nitroso-glutathione may, therefore, act as an intermediate NO donor in the inhibition of the IRK phosphorylation.

The finding that the various Cys $\rightarrow$ Ala mutant IRK proteins under test were equally susceptible to inhibition by NO is possibly explained by the assumption that the NO-mediated inhibition can be mediated by more than one cysteine residue. This possibility is supported by the three-dimensional simulation of the NO-induced structural changes. Three-dimensional modeling of protein structures by energy minimization is still regarded as a controversial method to predict the structural consequences of an alteration (*i.e.*, a mutation), which potentially affects the folding of the

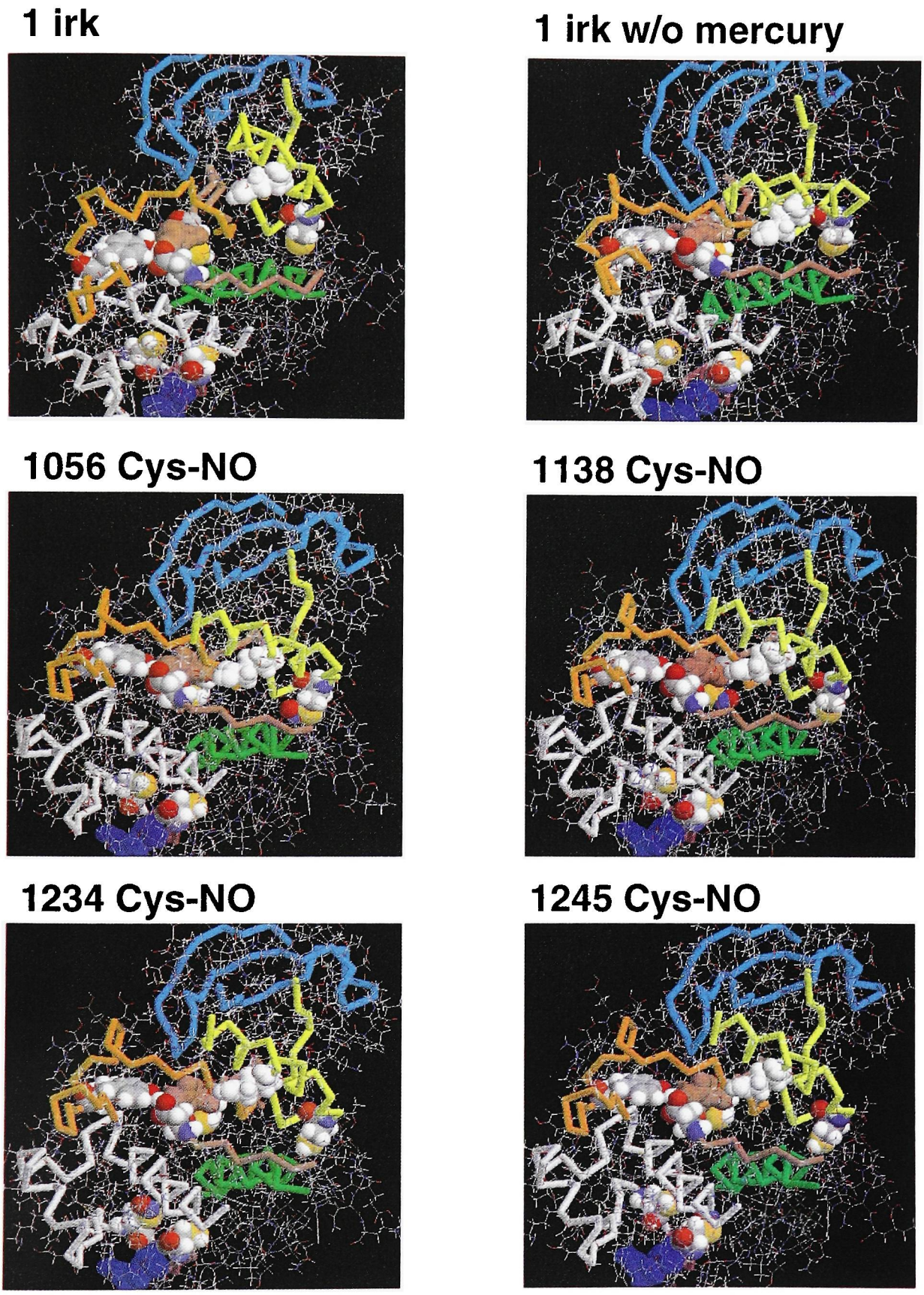

FIG. 5. Three-dimensional models of the original and *S*-nitrosylated β-IR. The view is upon the α-helix C. The β-IR structure is shown from a side opposite of the ATP binding site. The catalytic site with Tyr1162 is on the left side pointing to the center. For other details see legend to Fig. 4.

protein. However, this caveat does not apply to our three-dimensional modeling studies because energy minimization was used in this case to simulate moderate structural consequences of a post-translational modification of a protein that is already folded. The comparison of the six panels in Figs. 4 and 5 suggests that cysteine residues at four different positions of the IRK domain share the function of regulating the relative position of the two lobes. Because the lobe closure appears to facilitate the catalytic activation of the IRK by enhancing its accessibility for ATP (Hubbard, 1997), it is tempting to speculate that the inhibitory effect of NO may result from the NO-induced movement of the amino-terminal lobe in a direction opposite to the direction of lobe closure (*cf.* Hubbard, 1997). However, the role of other more subtle structural changes cannot be excluded. The most surprising result of our three-dimensional modeling studies was the finding that derivatization of any one of four different cysteine residues in four different regions of the molecule (illustrated in Figs. 4 and 5) leads to essentially the same structural changes. This is difficult to explain by chance coincidence and suggests strongly that the four cysteine residues 1056, 1138, 1234, and 1245 have essentially similar functions in the regulation of lobe orientation. This redundancy of functionally relevant cysteine residues is expected to increase the sensitivity to redox regulation by increasing the probability of redox interactions.

Taken together, our studies have shown that the initial IRK protein autophosphorylation, which is required for its catalytic activation and for insulin-dependent signal transduction, is subject to previously unknown regulatory events. Whether these regulatory events may contribute to the abnormally low IRK activity and accordingly low insulin responsiveness of the skeletal muscle tissue in obesity, non-insulin-dependent diabetes mellitus, and old age (Cahill, 1971; Friedenberg *et al.*, 1987; Takayama *et al.*, 1988; Fukagawa *et al.*, 1989; Damsbo *et al.*, 1991; Carvalho *et al.*, 1996) remains to be shown.

ACKNOWLEDGMENTS

The technical assistance of Mrs. Angelika Ott-Hartmann and Natalie Erbe and the assistance of Mrs. Ingrid Fryson in the preparation of this manuscript are gratefully acknowledged. This project was supported by a grant from the Deutsche Forschungsgemeinschaft (DR 66/7-1, DR 66/7-1).

REFERENCES

BECKER, K., GUI, M., and SCHIRMER, R.H. (1995). Inhibition of human glutathione reductase by S-nitrosoglutathione. Eur. J. Biochem. **234,** 472–478.

BÉDARD, S., MARCOTTE, B., and MARETTE, A. (1997). Cytokines modulate glucose transport in skeletal muscle by inducing the expression of inducible nitric oxide synthase. Biochem J. **325,** 487–493.

CAHILL, G.F., JR. (1971). The Banting memorial lecture 1971. Physiology of insulin in man. Diabetes **20,** 785–799.

CARVALHO, C.R., BRENELLI, S.L., SILVA, A.C., NUNES, A.L., VELLOSO, L.A., and SAAD, M.J. (1996). Effect of aging on insulin receptor, insulin receptor substrate-1, and phosphatidylinositol 3-kinase in liver and muscles of rats. Endocrinology **137,** 151–159.

CASELLI, A., CAMICI, G., MANAO, G., MONETI, G., PAZZAGLI, L., CAPPUGI, G., and RAMPONI, G. (1994). Nitric oxide causes inactivation of the low molecular weight phosphotyrosine protein phosphatase. J. Biol. Chem. **269,** 24878–24882.

DAMSBO, P., VAAG, A., HOTHER-NIELSEN, O., and BECK-NIELSEN, H. (1991). Reduced glycogen synthase activity in skeletal muscle from obese patients with and without type 2 (non-insulin-dependent) diabetes mellitus. Diabetologia **34,** 239–245.

ECK, H.-P., GMÜNDER, H., HARTMANN, M., PETZOLDT, D., DANIEL, V., and DRÖGE, W. (1989). Low concentrations of acid soluble thiol (cysteine) in the blood plasma of HIV-1 infected patients. Biol. Chem. Hoppe-Seyler **370,** 101–108.

ESTRADA, C., GÓMEZ, C., MARTIN-NIETO, J., DE FRUTOS, T., and JIMÉNEZ, A. (1997). Nitric oxide reversibly inhibits the epidermal growth factor receptor tyrosine kinase. Biochem. J. **326,** 369–376.

FREIDENBERG, G.R., HENRY, R.R., KLEIN, H.H., REICHART, D.R., and OLEFSKY, J. (1987). Decreased kinase activity of insulin receptors from adipocytes of non-insulin-dependent diabetic subjects. J. Clin. Invest. **79,** 240–250.

FUKAGAWA, N.K., MINAKER, K.L., YOUNG, V.R., MATTHEWS, D.E., BIER, D.M., and ROWE, J.W. (1989). Leucine metabolism in aging humans: effect of insulin and substrate availability. Am. J. Physiol. **256,** E288–E294.

GRIFFITH, O., and MEISTER, A. (1979). Potent and specific inhibitor of glutathione synthesis by buthionine sulfoximine (*S-n*-butyl-homocysteine sulfoximine). J. Biol. Chem. **254,** 7558–7560.

HAGLER, A.T., and LIFSON, S. (1974). Energy functions for peptides and proteins. II. The amide hydrogen bond

and calculation of amide crystal properties. J. Am. Chem. Soc. **96,** 5327–5335.

HUBBARD, S.R. (1997). Crystal structure of the activated insulin receptor tyrosine kinase in complex with peptide substrate and ATP analog. EMBO J. **16,** 5572–5581.

HUBBARD, S.R., WIE, L., ELLIS, L., and HENDRICKSON, W.A. (1994). Crystal structure of the tyrosine kinase domain of the human insulin receptor. Nature **372,** 746–754.

LANDER, H.M., SEHAJPAL, P., LEVINE, D.M., and NOVOGRODSKY, A. (1993). Activation of human peripheral blood mononuclear cells by nitric oxide-generating compounds. J. Immunol. **150,** 1509–1516.

LANDER, H.M., MILBANK, A.J., TAURAS, J.M., HAJJAR, D.P., HEMPSTEAD, B.L., SCHWARTZ, G.D., KRAEMER, R.T., MIRZA, U.A., CHAIT, B.T., BURK, S.C., and QUILLIAM, L.A. (1996). Redox regulation of cell signalling. Nature **381,** 380–381.

LEE, J., and PILCH, P.F. (1994). The insulin receptor: structure, function, and signaling. Am. J. Physiol. **266,** C319–C334.

LEI, S.Z., PAN, Z.-H., AGGARWAL, S.K., CHEN, H.-S.V., HARTMAN, J., SUCHER, N.J., and LIPTON, S.A. (1992). Effect of nitric oxide production on the redox modulatory site of the NMDA receptor-channel complex. Neuron **8,** 1087–1099.

MACAULAY, S.L., POLITES, M., FRENKEL, M.J., HEWISH, D.R., and WARD, C.W. (1995). Mutagenic structure/function analysis of the cytoplasmic cysteines of the insulin receptor. Biochem. J. **306,** 811–820.

MOLINA Y VEDIA, L., McDONALD, B., REEP, B., BRÜNE, B., DI SILVIO, M., BILLIAR, T.R., and LAPETINA, E.G. (1992). Nitric oxide-induced S-nitrosylation of glyceraldehyde-3-phosphate dehydrogenase inhibits enzymatic activity and increases endogenous ADP-ribosylation. J. Biol. Chem. **267,** 24929–24932.

SCHMID, E., EL BENNA, J., GALTER, D., KLEIN, G., and DRÖGE, W. (1998). Redox priming of the insulin receptor β-chain associated with altered tyrosine kinase activity and insulin responsiveness in the absence of tyrosine autophosphorylation. FASEB J. **12,** 863–870.

STAMLER, J.S. (1994). Redox signaling: Nitrosylation and related target interactions of nitric oxide. Cell **78,** 931–936.

STAMLER, J.S., SIMON, D.I., OSBORNE, J.A., MULLINS, M.E., JARAKI, O., MICHEL, T., SINGEL, D.J., and LOSCALZO, J. (1992). S-nitrosylation of proteins with nitric oxide: Synthesis and characterization of biologically active compounds. Proc. Natl. Acad. Sci. USA **89,** 444–448.

TAKAYAMA, S., KAHN, C.R., KUBO, K., and FOLEY, J.E. (1988). Alterations in insulin receptor autophosphorylation in insulin resistance: Correlation with altered sensitivity to glucose transport and antilipolysis to insulin. J. Clin. Endocrinol. Metab. **66,** 992–999.

TAYLOR, S.S., RADZIO-ANDZELM, E., and HUNTER, T. (1995). How do protein kinases discriminate between serine/threonine and tyrosine? Structural insights from the insulin receptor protein-tyrosine kinase. FASEB J. **9,** 1255–1266.

Address reprint requests to:
Dr. Wulf Dröge
Division of Immunochemistry
Deutsches Krebsforschungszentrum, D-69120
Heidelberg, Germany
E-mail: W.Droege@dkfz-heidelberg.de

This article has been cited by:

1. N WIERNSPERGER. 2005. Is non-insulin dependent glucose uptake a therapeutic alternative? Part 1: physiology, mechanisms and role of non insulin-dependent glucose uptake in type 2 diabetes. *Diabetes & Metabolism* **31**:5, 415-426. [CrossRef]